

# The Effect of Star Formation History on the Inferred Initial Stellar Mass Function

Bruce G. Elmegreen

*IBM Research Division, Yorktown Heights, New York 10598; email: bge@watson.ibm.com*

John Scalo

*Department of Astronomy, University of Texas, Austin, Texas 78712;  
e-mail: parrot@astro.as.utexas.edu*

## ABSTRACT

Peaks and lulls in the star formation rate (SFR) over the history of the Galaxy produce plateaux and declines in the present day mass function (PDMF) where the main-sequence lifetime overlaps the age and duration of the SFR variation. These PDMF features can be misinterpreted as the form of the intrinsic stellar initial mass function (IMF) if the star formation rate is assumed to be constant or slowly varying with time. This effect applies to all regions that have formed stars for longer than the age of the most massive stars, including OB associations, star complexes, and especially galactic field stars. Related problems may apply to embedded clusters. Evidence is summarized for temporal SFR variations from parsec scales to entire galaxies, all of which should contribute to inferred IMF distortions. We give examples of various star formation histories to demonstrate the types of false IMF structures that might be seen. These include short-duration bursts, stochastic histories with log-normal amplitude distributions, and oscillating histories with various periods and phases. The inferred IMF should appear steeper than the intrinsic IMF over mass ranges where the stellar lifetimes correspond to times of decreasing SFRs; shallow portions of the inferred IMF correspond to times of increasing SFRs. If field regions are populated by dispersed clusters and defined by their low current SFRs, then they should have steeper inferred IMFs than the clusters. The SFRs required to give the steep field IMFs in the LMC and SMC are determined. Structure observed in several determinations of the Milky Way field star IMF can be accounted for by a stochastic and bursty star formation history.

*Subject headings:* stars: formation—stars: mass function— Galaxy: stellar content— galaxies: starburst

## 1. Introduction

The star formation rate (SFR) in galaxies varies over a wide range of timescales. The ratio of recent to past-average SFR (denoted  $b$ ; see Scalo 1986) highlights the most recent changes. This ratio has been estimated using the equivalent width of  $H\alpha$  (Kennicutt, Tamblyn & Congdon 1994; Kennicutt 1998) and the ratio of far-infrared to blue luminosity (Tomita, Tomita, & Saito 1996), both of which suggest variations of up to an order of magnitude in galaxies of the same Hubble type. Related evidence for repetitive near-global bursts can be inferred from lopsided galaxies (Rudnick, Rix, & Kennicutt 2000), discrepancies between different SFR diagnostics (Sullivan et al. 2001), pixel-by-pixel models of disk galaxies at moderate redshifts (Glazebrook et al. 1999), and systematics of Tully-Fisher residuals for local galaxies (Kannappan, Fabricant, & Franx 2002). Recent work using much larger samples supports the idea that global variations are common in most galaxies: Salim et al. (2005) found SFR variations using GALEX UV and SDSS optical properties of 6500 galaxies, and Brinchmann et al. (2004) found them using optical emission lines in  $10^5$  SDSS galaxies. Related variations have been found in the  $H_2$ -to-HI ratio (Keres, Yun & Young 2003) and mass-to-light ratio (Roberts & Haynes 1994) for each Hubble type, and in the SFR for a given gas column density (Kennicutt 1998).

Population synthesis studies of nearby dwarf Irregulars also show a history of intense variations (Hunter 1997; Tolstoy et al. 1998; Hodge 1989; Carraro 2002; Grebel 2001; Van Zee 2001; Grebel & Gallagher 2004), while BCD galaxies are bursting today (Searle & Sargent 1972; Kunth & Ostlin 2000; Hopkins, Schulte-Ladbeck, & Drozdovsky 2002). Bursty SFR behavior in low-mass galaxies was found in the FORS Deep Field study of galaxies at redshift 1.5 (Bauer et al. 2005). The cause of most of these SFR variations is unknown, although some can be ascribed to tidal interactions between galaxies.

There is also evidence for SFR variations in the Milky Way. Stars in the solar neighborhood with ages up to several Gyr show SFR variations that have been interpreted as periodic or irregular (Barry 1988; Majewski 1993; Rocha-Pinto et al. 2000a,b; Hernandez, Valls-Gabaud, & Gilmore 2000; de la Fuente Marcos & de la Fuente Marcos 2004). Azimuthal orbit diffusion for ages more than a few  $10^8$  yr suggests these stars sample an entire annulus of our Galaxy (see Rocha-Pinto et al. 2000a). Thus the variations may be global.

Star formation events triggered by spiral density waves, swing amplified instabilities, and superbubbles have a timescale of  $\sim 10^8$  yrs. Gould’s Belt is an example of a local burst (Pöppel 1997). Another local burst  $2 - 4 \times 10^8$  yr ago was inferred from chromospheric ages (Barry 1988; Rocha-Pinto et al. 2000a,b), a bump in the present-day luminosity function (Scalo 1987), and a feature in the white dwarf luminosity function (Noh & Scalo 1990).

Compression and collapse from interstellar turbulence (see review in MacLow & Klessen 2004) and compression from the pressures of massive stars should lead to bursty star formation on a wide variety of spatial and temporal scales, including the small scales of cloud cores and clusters. For example, Hillenbrand (1997) and Palla & Stahler (2000, 2002) found an acceleration of SFRs in local star-forming regions over the last  $\sim 10^7$  yr, while Selman et al. (1999) found three large bursts in 30 Dor. A deceleration should occur when an active cloud core gets dispersed.

The purpose of this paper is to show the effect of these temporal variations on the present day mass function of stars, and to illustrate how the stellar initial mass function (IMF) can be erroneously derived if the detailed star formation rate history (SFH) is not properly included. The argument applies to all regions that have formed stars longer than the age of the most massive stars. Thus it applies to the inferred IMFs of OB associations, star complexes, very young clusters, and galactic field stars. It should also apply to the IMFs derived from luminosity functions inside young embedded clusters if the SFR varies during cluster formation. In these cases the SFH and IMF should be determined simultaneously, which requires ages and masses for stars from comparisons with isochrones (e.g. Hillenbrand 1997; Selman et al. 1999; Hillenbrand & Carpenter 2000; Muench et al. 2003). An additional complication occurs if the SFH depends on mass, i.e. if the massive stars form in different cloud cores than the low mass stars (e.g., DeGioia-Eastwood et al. 2001; see Elmegreen 2004).

The inferred IMF of an old cluster should not depend on the history of its formation if the most massive stars remaining in the cluster have main sequence lifetimes that are older than the duration of star formation in the cluster. Aside from evaporation and ejection, old clusters should show their correct intrinsic IMFs up to the most massive star that is still on the main sequence. The highest-mass part of the cluster IMF, which is now lost to stellar evolution, could have shown SFH-related deviations at an earlier stage if the cluster were observed then.

The global properties of galaxies such as integrated light and chemical abundances are also affected by the SFH. If large-scale bursts are as common as indicated, then models ignoring these bursts will derive the wrong PDMF even if the correct IMF is used. On the other hand, if there exists an intrinsic universal IMF whose form can be derived from open cluster studies (see Scalo 1998, 2005; Kroupa 2002), then our results imply that the SFH can be inferred from the PDMF. This technique was used by Scalo (1987) for the Milky Way, and Mighell & Butcher (1992) for the Carina dwarf spheroidal galaxy.

## 2. Inferred IMFs

The SFH,  $S(t)dt$ , combined with the intrinsic IMF,  $f(M)d\log M$ , gives the PDMF  $\phi(M)d\log M$ ,

$$\phi(M) = f(M) \int_0^{t(M)} S(t)dt \quad (1)$$

where  $t(M)$  is the main-sequence lifetime of a star of mass  $M$ . In this equation, the age  $t$  increases into the past from the present time at  $t = 0$ . We assume  $f(M)$  is independent of time and measured in log-intervals of stellar mass. Only the relative variations in the star formation rate,  $S(t)$ , have an effect on the IMF; the absolute SFR does not matter. Thus the IMF modulations we discuss here apply to all regions where stars have formed with a relative rate of  $S(t)$  and a time-invariant intrinsic IMF  $f(M)$  of any type. We do not consider time-variable intrinsic IMFs in our examples, but such variations could be present in galaxies as well.

The PDMF is not observed directly but inferred from the luminosity function using a mass-luminosity relation. This procedure can be used only for groups of stars in the main sequence phase of evolution: the mass-luminosity relation is not one-to-one for pre-main sequence stars. Usually the field or galactic average IMF is derived from the PDMF by assuming a SFH that varies smoothly over large timescales. For our example, a constant SFH,  $S_0$ , would give an inferred IMF  $f_{infer}(M) = \phi(M)/[S_0 t(M)]$ . For the approximation  $t(M) \sim M^{-2.2}$  (Mihalas & Binney 1981), this gives  $f_{infer}(M) \propto \phi(M)M^{2.2}$ .

Structure in the inferred IMF comes from unknown variations in  $S(t)$ . This structure may be derived analytically for simple burst cases of  $S(t)$ , which include a sudden increase followed by an exponential or power-law decline, or a sinusoidal variation. These analytically solvable cases can be used to show that the amplitude and mass range of the resulting features in  $f_{infer}$  are determined primarily by the age, duration, and amplitude of the burst in  $S(t)$ . The shapes of the features are relatively insensitive to the precise form of  $S(t)$  for these burst cases.

In the models below, the intrinsic IMF is assumed for illustrative purposes to be  $f(M) \propto M^\Gamma$  for  $M > 1 M_\odot$  with  $\Gamma = -1.5$ , a value that brackets empirical estimates ( $\Gamma = -1.35$  is the Salpeter IMF slope; see review in Chabrier 2003). Different  $\Gamma$  introduce different tilts in the inferred IMF without changing the form of the IMF distortions. The IMF below  $1 M_\odot$  is not included because such stars live longer than  $10^{10}$  yr, the longest age considered here. The conversion between mass and main sequence lifetime is assumed to be given by the fit to the models of Schaller et al. (1992) in Reid, Gizis & Hawley (2002):

$$\log_{10}(t) = 10.015 - 3.461 \log_{10}(M) + 0.8157 \log_{10}(M)^2. \quad (2)$$

Figure 1 shows the effect of a delta-function burst of star formation on the inferred IMF if  $S(t)$  is erroneously assumed to be constant. On the left is the dimensionless SFH (with each case displaced upward for clarity), and on the right is the inferred IMF made under this erroneous assumption. The actual SFH is taken to be a constant value of 1 except in bursts where it increases by a factor of 10. Features in the inferred IMFs occur at each mass where the main-sequence time equals the burst time. If the IMF is divided by the intrinsic IMF,  $M^\Gamma$ , and the derivative taken, then the SFH will be recovered (see Eq. 5 below). Note that the inferred IMF is exactly the intrinsic IMF at masses above the main-sequence turn off mass for the burst age because these massive stars were not around at the time of the burst. The IMF flattens just below the turnoff mass because some of these stars formed in the burst. For bursts with a finite duration, the sharp drop in the inferred IMF above the turnoff mass would be broadened.

The inferred IMF is plotted up to  $100 M_\odot$  in all of the figures even though the galactic IMF is not well known above  $\sim 50 M_\odot$  and may not be a continuation of the assumed power law from lower masses. In addition, the highest-mass stellar lifetimes are comparable to the shortest timescales for variations considered here, so there are no features in any of our inferred IMFs above  $\sim 50 M_\odot$ . Nevertheless, the plotting is done in this way to give a high-mass baseline for viewing the IMF variations at lower mass.

Figures 2-5 show other inferred IMFs for various star formation histories. Figure 2 has dimensionless SFHs that are made from the exponentiation of the Fourier transform of noise that was multiplied by  $k^{-\beta}$  for wavenumber  $k$ . We make these stochastic SFHs in the following way (see also Weinberg & Cole 1992 for cosmological applications and Elmegreen 2002 for applications to cloud mass functions). We first generate 5000 random numbers  $R_1$  and another 5000  $R_2$  with values uniformly sampled between  $-0.5$  and  $0.5$ . Then we take the Fourier transform of  $k^{-\beta}$  times these random numbers, using integers for  $k$  between 1 and 5000 and integers for time  $t$  between 1 and  $10^4$ . The units of  $t$  are My. This gives

$$F(t) = \sum_{k=1}^{5000} k^{-\beta} (R_1(k) \sin [\omega kt] + R_2(k) \cos [\omega kt]) . \quad (3)$$

Finally, we take for the SFH the exponentiation of this result:

$$S(t) = \exp (F [t]) \quad (4)$$

The frequency is  $\omega = 2\pi / (10^4 My)$ . The multiplication of the noise by  $k^{-\beta}$  for  $\beta = 0.25$ ,  $0.5$ , and  $1$  makes the power spectrum of  $F(t)$  a power-law with a slope of  $-0.5$ ,  $-1$ , and  $-2$ , respectively. The amplitudes of  $F(t)$  have a Gaussian pdf, so the exponentiation of  $F(t)$

gives  $S(t)$  a log-normal pdf. Because transformation of the one-point pdf can distort the power spectrum, we checked the power spectrum before and after exponentiation and found little difference aside from an amplitude shift, and therefore did not apply the correction described by Weinberg & Cole (2001). The corresponding SFHs are plotted in the bottom, middle, and top panels, respectively. The rms dispersion of  $F(t)$  is normalized to 1 in each case (not shown in the equations above), and the average value of  $F(t)$  is normalized to 0.1 for the lower SFH in each panel, 1 for the middle, and 10 for the upper. Note that the vertical scales differ for each curve in a panel; the normalization of the average  $F(t)$  does not affect the inferred IMF. As a result of these steps,  $S(t)$  has a log-normal pdf and an approximately power-law power spectrum. The fat tail of the log-normal pdf provides the intermittency that is meant to mimic the short bursts and longer lulls expected from turbulent density variations in the ISM.

Figure 3 shows 11 different random-number renditions of the same stochastic history model used for the middle curve in the middle panel of Figure 2. That is, the power-law slope in Figure 3 is  $-1$  and the normalized average of  $F(t)$  is 1. The inferred IMFs vary a lot from curve to curve, reflecting the different details in the SFHs plotted on the left. These variations would be greater or smaller for SFHs with power spectra of  $-2$  or  $-0.5$ , respectively, as can be inferred from Figure 2. Stochastic effects like this could be responsible for some of the structure seen in the field star initial mass function when the range of masses is large and the IMF features are not smoothed by large mass bins. Examples are the ledges and dips in the IMF by Scalo (1986, Fig. 16), Rana (1991, Fig. 3), and Basu & Rana (1992, Fig. 6). Structure can even be seen in Salpeter’s (1955) IMF. Of course these features could also be due to structure in the functions needed to transform from the PDMF to the IMF (see Scalo 1986), or they could be intrinsic to the IMF. Unfortunately, the most recent determinations of the field star IMF (Reid, Gizis, & Hawley 2002; Schroder & Pagel 2003) do not cover a large enough range in mass above  $1 M_{\odot}$  for such structure to be noticed. Future studies of the intermediate-mass IMF that include a larger mass range should find the predicted signatures of SFH variations.

Figure 4 has sinusoidal SFHs with various phases shown on the left. Each sine function has a constant added so that zero is the minimum value of the star formation rate in the bottom two left panels, with a full range from 0 to 2, and 0.5 is the minimum value in the top left panel, with a range from 0.5 to 1.5. This top panel in Figure 4 shows the effect of diluting the sinusoidal variation with a constant minimum SFR. The bumps in the IMF on the right are correspondingly weaker for this diluted case than they are in the bottom two panels. This difference illustrates how the relative amplitude of the SFH variations control the magnitude of the IMF effect.

Figure 4 indicates that the intermediate-to-high mass part of the IMF can become very steep if the SFH declines continuously to the present day. This is the case in the middle panel for the sine function having a value of 0 at  $t = 0$  (the blue curve). The figure also shows how the IMF is hardly affected below the mass whose main sequence lifetime equals the period of the sinusoidal variation of the SFH. This is because lower mass stars form during many periods of the variation so the ups and downs of the SFH average out to a nearly steady star formation rate.

In Figure 5, the inferred IMFs (right hand side) and IMF slopes at 5, 10, and 20  $M_{\odot}$  (top left) are plotted versus the phase from the sinusoidal model in the lower left. The phase is measured relative to  $2\pi$ , which is a full cycle of the sinusoid. The inferred IMF is distorted in a way that depends on the current phase in the star formation variation. An example was previously noted for Figure 4: if the most recent SFR has declined sharply to a value of zero today (as for the green curve in the lower left panel of Fig. 5), then the inferred IMF would have a relatively steep slope from intermediate to high mass (corresponding to the green and lower curve in the right-hand panel). Or, if the SFR had its most recent minimum 25 My ago and then started to rise again (red curve on the lower left), then the inferred IMF would have a dip at the mass whose main-sequence lifetime is 25 My (red line on the right). The phase of the sinusoid in the first example is 0, and the IMF slopes at 5, 10, and 20  $M_{\odot}$  are  $-3.8$ ,  $-5.0$  and  $-3.9$ , as shown in the top left panel for phase= 0. The phase in the second example is  $1/8$  of  $2\pi$ , and the IMF slopes at these three masses are  $-6.5$ ,  $0.3$ , and  $-1.09$ , respectively, as shown in the top left for phase= 0.125. In general, the time of the most recent significant dip in the SFR should correspond to the stellar main sequence life time at the mass where there is a corresponding dip in the IMF.

Star formation histories like these are not unreasonable. In a galaxy with irregular spiral structure and star formation triggered stochastically by turbulent compression, one might expect the star formation rate to vary with a power spectrum that is related to the power spectrum of the local dynamical rate. If the local dynamical rate is proportional to the square root of density, and the density has a log-normal pdf as in isothermal turbulence simulations (e.g., Li, Klessen & Mac Low 2003), then our SFH in Figure 2 follows. Lower  $\beta$  corresponds to relatively more short-period SFR variations, which shifts the irregularities in the inferred IMF toward higher mass while averaging over and reducing the IMF variations at lower mass.

In a galaxy with global periodic triggering or organization of star formation by a spiral density wave, the SFH can have periodic variations. The periods used in Figure 4 are 20 My for the bottom panel and 200 My for the middle and top panel. The short period hardly shows up in the inferred IMF because most stars live longer than that. The long period,

which is comparable to the time between spiral arm passages at typical mid-disk positions, gives a clear signature in the inferred IMF. This signature can make the intermediate to high mass slope steeper than the intrinsic slope if the surveyed stars are down stream from the arm and the SFH has recently declined (Fig. 5). There is no symmetry for stars upstream. Far upstream the field stars reflect the previous arm passage. At the point where the SFR strongly increases, most star forming regions will still be young and in clusters.

### 3. Steep IMFs Inferred for the Field Regions of the LMC and SMC

The figures illustrate what happens in regions of galaxies where the SFR has varied. The observed population is always a PDMF, so equation 1 has to be applied to obtain the IMF. If, for example, a decline in the SFR is not included in the derivation of the IMF from the PDMF, then the inferred IMF will be relatively steep down to the mass where the turnoff age equals the age at the beginning of the decline.

The remote field regions of the LMC and SMC may be examples. They have low SFRs compared to their recent past or else they would be still be OB associations. Thus, one might expect the inferred IMFs to be steeper than the intrinsic IMF if the SFR is incorrectly assumed to be constant. This could explain some of the effect found by Massey and collaborators (e.g., Massey et al. 1995; Massey 2002) who assumed a constant SFR for LMC and SMC fields and derived  $\Gamma \sim -4 \pm 0.5$  in the mass range 25–120  $M_{\odot}$ . A decline in the SFR over the last  $\sim 5$  My could explain this  $\Gamma$  (using Eq. 2) even if the intrinsic IMF had the Salpeter slope when the observed stars formed. The question is, how large does the decline have to be and is such a decline reasonable for the whole LMC?

The steep slope found by Massey et al. is steeper than that obtained for the field regions of the LMC by other groups, and in the Massey et al. studies it primarily applies to the highest masses. For example, Massey (2002) divided his star counts into 4 mass bins in Table 12: for the two lowest bins, covering masses from 25–60  $M_{\odot}$ , the inferred IMF slope is  $\Gamma = \Delta \log \xi / \Delta \log(M) = -2.2$ ; for the two intermediate mass bins, covering 40–85  $M_{\odot}$ ,  $\Gamma = -6.2$ , and for the two highest mass bins, covering 60–120  $M_{\odot}$ ,  $\Gamma = -2.6$ . Evidently, the overall  $\Gamma \sim -4$  is steep because of the very steep drop between 40 and 85  $M_{\odot}$ . The statistical uncertainty in this result is large, however; for the LMC there are only 16 stars in the two highest mass bins, while there are 835 stars in the 2 lowest mass bins; for the SMC, which has the same  $\Gamma_{infer}$  overall, there are 5 and 284 stars in these bins, respectively. Parker et al. (1998) obtained  $\Gamma \sim -1.8 \pm 0.09$  for the 7–35  $M_{\odot}$  mass range among 26713 LMC field stars observed with the Ultraviolet Imaging Telescope, suggesting that steepening at smaller masses is marginal. The statistical uncertainty in the Parker et al. result is remarkably low;

they assumed continuous star formation in converting the luminosity function to an IMF.

The PDMF for the LMC field observed by Gouliermis et al. (2005) is  $\propto M^{-6}$  at low mass ( $0.9\text{--}2\text{ M}_\odot$ ) and  $M^{-3.7}$  for the whole mass range ( $0.9\text{--}6\text{ M}_\odot$ ). They comment that the PDMF for the lowest mass range should equal the IMF because there should be little evolution at such low masses. In fact the lifetime of a  $2\text{ M}_\odot$  star is only 1 Gy according to equation 2, so there is still time for the SFH to be important if the LMC disk has an age comparable to that of the Milky Way,  $\sim 10\text{ Gy}$ . Then the PDMF should be divided by  $t(M)$  to get the inferred IMF. For the lower mass range,  $t(M) \sim M^{-3.3}$  using equation (2), and if the SFH is uniform, the resulting IMF is  $\propto M^{-2.7}$ . The full mass range should be corrected for  $t(M) \sim M^{-2.9}$  from equation (2), giving an IMF  $\propto M^{-0.8}$ . The Gouliermis et al. result is interesting because it suggests the steep IMF inferred for the field (under the assumption of a constant SFR) may continue in some regions all the way down to  $\sim 1\text{ M}_\odot$ .

These studies allow for the possibility that the LMC and SMC field IMFs at masses above  $\sim 40\text{ M}_\odot$  are steeper than the field IMFs at intermediate masses, and that both of these are steeper than what is found in LMC clusters and associations (e.g. Kroupa 2002; Sirianni et al. 2000; Parker et al. 2001; Gouliermis et al. 2005). The implication that dense regions systematically form proportionally more massive stars than low-density regions was explored by Elmegreen (2004). However, the results of the present paper suggest a new explanation for steep field IMFs that is independent of physical processes during star formation. In this explanation, the field stars are dispersed clusters or other stars with an *intrinsically* shallow (cluster-like) IMF, but they occur in places where the SFR has been declining for a time equal to the lifetime of the lowest mass star on the steep part of the *inferred* IMF.

Figure 6 shows various constraints on the SFH required to produce a steep inferred IMF from this model alone. It was obtained by inverting equations (1) and (2). This was done in two steps: first the PDMF,  $\phi(M)$ , was recovered from the inferred IMF,  $f_{infer}$ , and stellar lifetime function,  $t(M)$ , using a constant SFR,  $S_0$ , as assumed by Massey (2002) and others:  $\phi(M) = f_{infer}(M)S_0t(M)$ . Then equation 1 was rewritten as  $\phi(M)/f(M) = \int_0^{t(M)} S(t)dt$  for intrinsic IMF  $f$  and differentiated on both sides with respect to  $M$ . After rearrangement, this gives

$$\frac{S(t)}{S_0} = \frac{d(f_{infer}t/f)/dM}{dt/dM} = \frac{f_{infer}}{f} + \frac{d(f_{infer}/f)/dM}{d \ln t/dM}. \quad (5)$$

The figure uses an intrinsic IMF with  $\Gamma = -1.35$  (the Salpeter IMF) and three values of an inferred IMF slope  $\Gamma_{infer} = -4, -3$ , and  $-2$ . The Salpeter slope was used for illustration; the results would be similar for other power-laws. For each of these  $\Gamma_{infer}$ , two SFHs are given, one decreasing continuously over the past 10 Gy (dotted line), which gives  $\Gamma = \Gamma_{infer}$  for all masses  $> 1\text{ M}_\odot$ , and another decreasing only for the last 20 My (solid line), which

gives  $\Gamma = \Gamma_{infer}$  above  $10 M_{\odot}$  and  $\Gamma = -1.35$  for lower  $M$ . The fiducial slopes for inferred and intrinsic IMFs are shown by the dashed lines. If these examples apply to the field regions of the LMC and SMC for masses above  $10 M_{\odot}$ , for example, then the SFR had to drop there by factors of 63, 9.2, and 1.9, respectively, during the last  $\sim 20$  My. For  $\Gamma = -1.8$  between 7 and  $35 M_{\odot}$  observed by Parker et al., the required SFR drop is 1.6 in 47 My, the lifetime of a  $7 M_{\odot}$  star. Such drops would not be unreasonable if the field regions were sites of dense clouds and star formation  $\sim 50 - 20$  My ago, and these clouds have since dispersed and moved elsewhere by the pressures of young stars.

Models of star formation in the LMC suggest the overall rate has decreased steadily for the last  $\sim 1$  Gy, following a large burst at about that time in the past (Bertelli et al. 1992; Westerlund, Linde, & Lyng 1995; Vallenari et al. 1996; Gallagher et al. 1996). While the details of this decline are uncertain, this is the type of SFH that could explain a moderately steep ( $\Gamma \sim -2$ ) field IMF down to  $\sim 2 M_{\odot}$ . For the three assumed values of  $\Gamma_{infer} = -4$ ,  $-3$ , and  $-2$  in Figure 6, the SFR drops over the last Gy by factors of 3780, 112, and 5.0. Gallagher et al. allow for a factor of  $\sim 3$  decrease in the SFR over the last Gy. Thus a declining SFR in the LMC could explain the moderately steep field IMF inferred by Parker et al. (1998) and others, even down to  $\sim 2 M_{\odot}$  if needed. That is, the factor of  $\sim 5$  drop in SFR over 1 Gy suggested for our  $\Gamma = -2$  case in Figure 6 is about the same as the factor of  $\sim 3$  drop observed by Gallagher et al. for 1 Gy. More precisely, for the  $\Gamma_{infer} = -1.8$  obtained by Parker et al., the SFR has to drop by a factor of 2.6 over 1 Gy; this is almost the same as the drop observed by Gallagher et al.. Gallagher et al. also rule out a drop in the SFR by more than a factor 10 in the last 0.1 Gy. This is consistent with the Massey et al. result of  $\Gamma_{infer} \sim -4$  for  $M > 40 M_{\odot}$  because that requires a drop of a factor of  $\sim 3.3$  over the last 3.7 My, the lifetime of a  $40 M_{\odot}$  star according to equation 2.

Other models for steep field  $\Gamma$ 's include a greater dispersal from OB associations of low-mass stars compared to high mass stars resulting from the longer lives of the low mass stars (Elmegreen 1997, 1999; Hoopes, Walterbos & Bothun 2001; Tremonti et al. 2002), a dependence of maximum stellar mass on cluster mass that is either the result of statistical sampling effects (Kroupa & Weidner 2003) or in addition to these effects (Elmegreen 1999), the evaporation of cluster halos that have a steep IMF from birth (e.g., de Grijs et al. 2002), and inadequate corrections for low-mass background stars (Parker et al. 2001). Field contamination by runaway stars that are the minor companions of binaries can steepen the IMF too. All of these processes, in addition to decelerating star formation, can steepen both the PDMF and the inferred field IMF while allowing a somewhat shallow, cluster-like, intrinsic IMF.

#### 4. Conclusions

Variations in the star formation rate over times from  $\sim 2 \times 10^6$  to  $10^9$  yr, as expected from observations of our own and other galaxies, can produce variations in the slope of the present day mass function that will be misinterpreted as variations in the slope of the IMF if the star formation history is assumed to vary more smoothly or not at all. The resulting IMFs can have false flattenings or steepenings at masses whose main sequence age is comparable to the time since the star formation event. IMF steepening can be large if star formation turns off suddenly.

Applications of these results to the field regions of the LMC and SMC appear promising. There the inferred IMF is relatively steep for intermediate mass stars,  $\Gamma \sim -1.8$  compared to a Salpeter slope of  $-1.35$ , and even steeper for high mass stars,  $\Gamma \sim -4$  for  $M > 40 M_\odot$ . We found that the  $\Gamma \sim -1.8$  observation by Parker et al. (1998) between 7 and  $35 M_\odot$  could result from a decline in the average star formation rate by a factor of 1.6 over the last 47 My if the intrinsic IMF is the Salpeter function. Similarly, the  $\Gamma \sim -4$  observation by Massey (2002) for  $M > 40 M_\odot$  could result from a decline by a factor of 3.3 over the last 3.7 My. If  $\Gamma = -1.8$  all the way down to  $2 M_\odot$ , then the required decline would be a factor of 2.6 over the last 1 Gy. These declines would have had to occur throughout the entire LMC and SMC if the inferred steep IMFs are the same in all field regions. If this is the case, then the field stars could be from dispersed clusters where the intrinsic IMF was relatively shallow at birth.

Our results apply also to IMF determinations of young clusters with a substantial pre-main sequence population if the IMF is estimated from the luminosity function. That problem is more complicated than the cases modeled here because there is no one-to-one relation between mass and luminosity for pre-main sequence stars. In order to obtain a reliable IMF for pre-main sequence stars, the SFH should be determined simultaneously with the IMF using theoretical isochrones in the H-R diagram – a procedure that has been used by several groups but can still introduce systematic errors if there are uncertainties in the isochrones and effective temperature scale. Older clusters should not have a problem with their inferred IMFs if the main sequence lifetime of the most massive star is longer than the length of time during which the cluster formed.

Applications of SFH variations to the field IMF are additionally complicated by the fact that the present local field population consists of stars with a wide range of ages that originated in diverse parts of the Galaxy having different SFHs. The range of birth sites increases with decreasing mass because main sequence lifetime and mean age increase with decreasing mass. The range in birthplace distance is the result of stellar orbit diffusion, which is rapid in the azimuthal direction, increasing with the square root of the stellar age (Wielen

1977; see Rocha-Pinto et al. 2004 for a review of processes). Radial mixing by stellar waves was recently studied by Sellwood & Binney (2002). Because there is a wide range of birth distances for stars spanning the inferred field IMF, many different SFR histories are involved. We neglected this effect here. For stars that are too young for significant orbit diffusion (ages less than a few  $10^8$  yr), this neglect is equivalent to assuming that all SFR variations are coherent over spatial scales larger than the stellar age times the average velocity dispersion. In principle, the age spread of solar neighborhood stars with a given mass can significantly affect the inferred IMF if each star comes from a region with a different SFH. For this reason it will be difficult to infer any intrinsic IMF from field stars without detailed models of their migration into the local neighborhood and their spatial and temporal distribution of formation rates.

Helpful comments by the referee are gratefully acknowledged. JMS acknowledges support through NASA ATP Grant NAG5-13280.

## REFERENCES

- Barry, D.C. 1988, *ApJ*, 334, 436
- Basu, S. & Rana, N. C. 1992, *ApJ*, 393, 373
- Bauer, A. E., Drory, N., Hill, G. J., & Feulner, G. 2005, *ApJL*, 621, L89.
- Bertelli, G., Mateo, M., Chiosi, C., & Bressan, A. 1992, *ApJ*, 388, 400
- Brinchmann, J., Charlot, S., White, S. D. M., Tremonti, C., Kauffmann, G., Heckman, T., & Brinkmann, J. 2004, *MNRAS*, 351, 1151
- Carraro, G. 2002, in *Modes of Star Formation and the Origin of Field Populations*, ASP Conference Series 285, ed. E.K. Grebel & W. Brandner, p. 358
- Chabrier, G. 2003, *PASP*, 115, 763
- DeGioia-Eastwood, K. Throop, H., & Walker, G. 2001, *ApJ*, 549, 578
- de Grijs, R., Gilmore, G. F., Johnson, R. A., & Mackey, A. D. 2002, *MNRAS*, 331, 245
- de La Fuente Marcos, R., & de La Fuente Marcos, C. 2004, *New Astron.*, 9, 475
- Elmegreen, B.G. 1997, *ApJ*, 486, 944
- Elmegreen, B.G. 1999, *ApJ*, 515, 323

- Elmegreen, B.G. 2002, ApJ, 564, 773
- Elmegreen, B.G. 2004, MNRAS, 354, 367
- Gallagher, J. S., et al. 1996, ApJ, 466, 732
- Glazebrook, K., Blake, C., Economou, F., Lilly, S., Colless, M., 1999, MNRAS, 306, 843
- Gouliermis, D., Brandner, W., & Henning, Th. 2005, *astroph/0411448v2*
- Grebel, E.K. 2001, Ap&SS, 277, 231
- Grebel, E.K., & Gallagher, J.S., III. 2004, ApJL, 610, 89
- Hernandez, X., Valls-Gabaud, D., & Gilmore, G. 2000, MNRAS, 316, 605
- Hillenbrand, L.A. 1997, AJ, 113, 1733
- Hillenbrand, L. A., & Carpenter, J. M. 2000, ApJ, 540, 236
- Hodge, P. 1989, ARA&A, 27, 139
- Hoopes, C.G., Walterbos, R. A. M., Bothun, G.D. 2001, ApJ, 559, 878
- Hopkins, A. M., Schulte-Ladbeck, R. E., & Drozdovsky, I. O. 2002, AJ, 124, 862
- Hunter, D.A. 1997, PASP, 109, 937
- Kennicutt, R.C. Jr., 1998, ApJ, 498, 541
- Kennicutt, R.C., Jr., Tamblyn, P., & Congdon, C.W. 1994, ApJ, 435, 22
- Keres, D., Yun, M.S., & Young, J. S. 2003, ApJ, 582, 659
- Kannappan, S.J., Fabricant, D.G., & Franx, M. 2002, AJ, 123, 2358
- Kroupa, P. 2002 Science, 295, 82
- Kunth, D., & Ostlin, G. 2000, A&ARev. 10, 1
- Li, Y., Klessen, R.S., Mac Low, M.-M. 2003, ApJ, 592, 975
- Majewski S.R., 1993, ARA&A, 31, 575
- Mac Low, M.-M., Klessen, R.S. 2004, Rev. Mod. Phys., 76, 125
- Massey, P. 2002, ApJS, 141, 81

- Massey, P., Lang, C. C., DeGioia-Eastwood, K., & Garmany, C. D. 1995, *ApJ*, 438, 188
- Mighell, K.J. & Butcher, H.R. 1992, *A&A*, 255, 26
- Mihalas, D. & Binney, J. 1981, *Galactic Astronomy* San Francisco: Freeman, p. 113
- Muench, A. A., Lada, E. A., Lada, C. J., Elston, R. J., Alves, J. F., Horrobin, M., Huard, T. H., Levine, J. L., Raines, S. N., & Roman-Zuniga, C. 2003, *ApJ*, 125, 2029
- Noh, H.-R. & Scalo, J.M. 1990, *ApJ*, 352, 605
- Palla, F., & Stahler, S. W. 2000, *ApJ*, 540, 255
- Palla, F., & Stahler, S. W. 2002, *ApJ*, 581, 1194
- Parker, J.W., Hill, J.K., Cornett, R.H., Hollis, J., Zamkoff, E., Bohlin, R. C., O’Connell, R.W., Neff, S.G., Roberts, M.S., Smith, A.M. & Stecher, T.P. 1998, *AJ*, 116, 180
- Parker, J.W., Zaritsky, D., Stecher, T.P., Harris, J., & Massey, P. 2001, *AJ*, 121, 891
- Pöppel, W. 1997, *Fundamentals of Cosmic Phys.*, 18, 1
- Rana, N. C. 1991, *ARA&A*, 29, 129
- Reid, I. N., Gizis, J. E., Hawley, S.L. 2002, *AJ*, 124, 2721
- Roberts, M.S., & Haynes, M.P. 1994, *ARAA*, 32, 115
- Rocha-Pinto, H. J., Scalo, J., Maciel, W. J. & Flynn, C. 2000a, *A&A*, 358, 869
- Rocha-Pinto, H.J., Scalo, J., Maciel, W.J., Flynn, C. 2000b, *ApJL*, 531, 115
- Rocha-Pinto, H. J., Flynn, C., Scalo, J., Hanninen, J., Maciel, W. J., & Hensler, G. 2004, *A&A* 423, 517
- Rudnick, G., Rix, H.-W., & Kennicutt, R.C. 2000, *ApJ*, 538, 569
- Salim, S. et al. 2005, *ApJL*, 619, 39
- Scalo, J. M. 1986, *Fund. Cos. Phys.*, 11, 1
- Schaller, G., Schaerer, D., Meynet, G., & Maeder, A. 1992, *A&AS*, 96, 269
- Scalo J.M., 1986, *Fundamentals Cosmic Phys.*, 11, 1

- Scalo, J. M. 1987, in *Galaxy Evolution*, Tenth European Astronomy Meeting of the IAU, vol. 4, ed. J. Palous, p. 101.
- Scalo, J.M. 1998, in *The Stellar Initial Mass Function*, ed. G. Gilmore & D. Howell, ASP Conference Series, Vol. 142, p.201
- Scalo, J.M. 2005, in *IMF@50: The Stellar Initial Mass Function Fifty Years Later*, ed. E. Corbelli, F. Palla, & H. Zinnecker, Dordrecht: Kluwer, in press
- Schroder, K.-P., & Pagel, B. E. J. 2003, *MNRAS*, 343, 1231
- Searle, L., & Sargent, W. L. W. 1972, *ApJ*, 172, 25
- Sellwood, J.A., & Binney, J.J. 2002, *MNRAS*, 336, 785
- Selman, F., Melnick, J., Bosch, G., & Terlevich, R. 1999, *A&A*, 347, 532
- Sirianni, M., Nota, A., Leitherer, C., De Marchi, G., & Clampin, M. 2000, *ApJ*, 533, 203
- Sullivan, M., Mobasher, B., Chan, B., Cram, L., Ellis, R., Treyer, M., & Hopkins, A. 2001, *ApJ*, 558, 72
- Tomita, A., Tomita, Y., & Saito, M. 1996, *PASJ*, 29, 71
- Tolstoy, E., Gallagher, J. S., Cole, A. A., Hoessel, J. G., Saha, A., Dohm-Palmer, R. C., Skillman, E. D., Mateo, M., Hurley-Keller, D. 1998, *ApJ*, 116, 1244
- Tremonti, C.A., Calzetti, D., Leitherer, C., & Heckman, T.M. 2002, *ApJ*, 555, 322
- Van Zee, L. 2001, *AJ*, 121, 2003
- Wielen, R. 1977, *A&A*, 60, 263
- Weinberg, D.H., & Cole, S. 1992, *MNRAS*, 259, 652

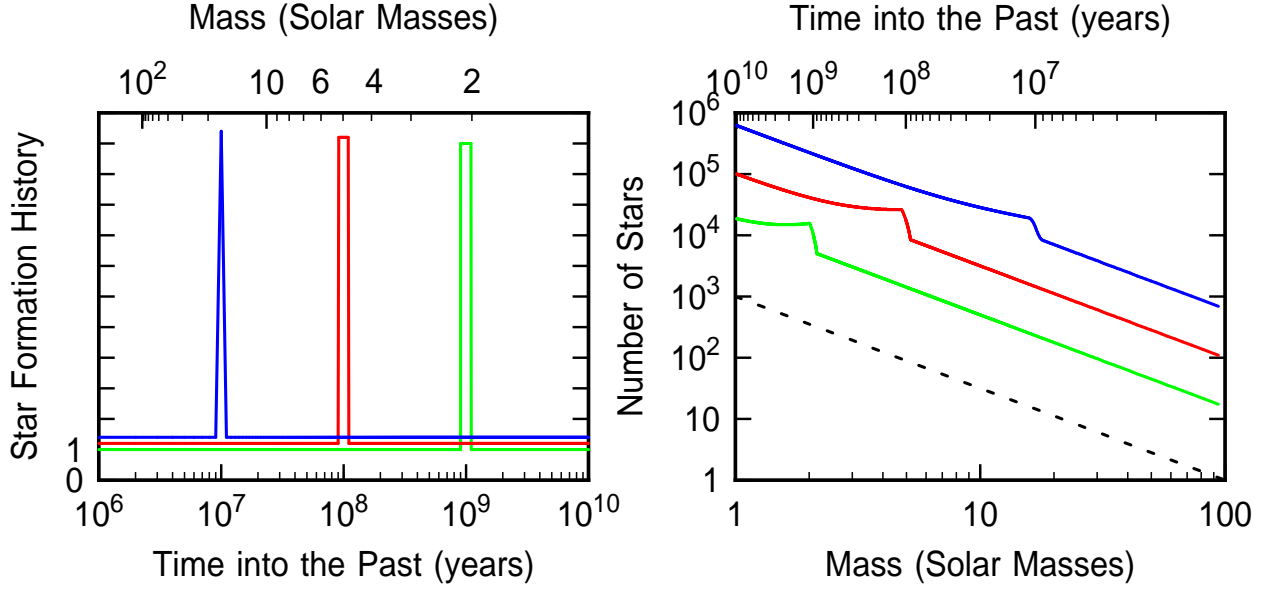


Fig. 1.— (left) Three sample star formation histories consist of a constant rate with a burst at various times. Present time is to the left. Successive plots are shifted upward for clarity. The masses whose main sequence lifetimes correspond to the ages on the abscissa are indicated on the top axis. The corresponding present day mass functions derived from these SFHs were divided by the main-sequence age as a function of mass to give the inferred IMFs on the right. These would be the IMFs inferred for the region if the star formation rate were erroneously taken to be constant. The inferred IMFs have features at masses where the main sequence ages equal the burst times. The main sequence lifetime for each mass is indicated on the top axis. The dotted line has the intrinsic IMF slope of  $\Gamma = -1.5$ .

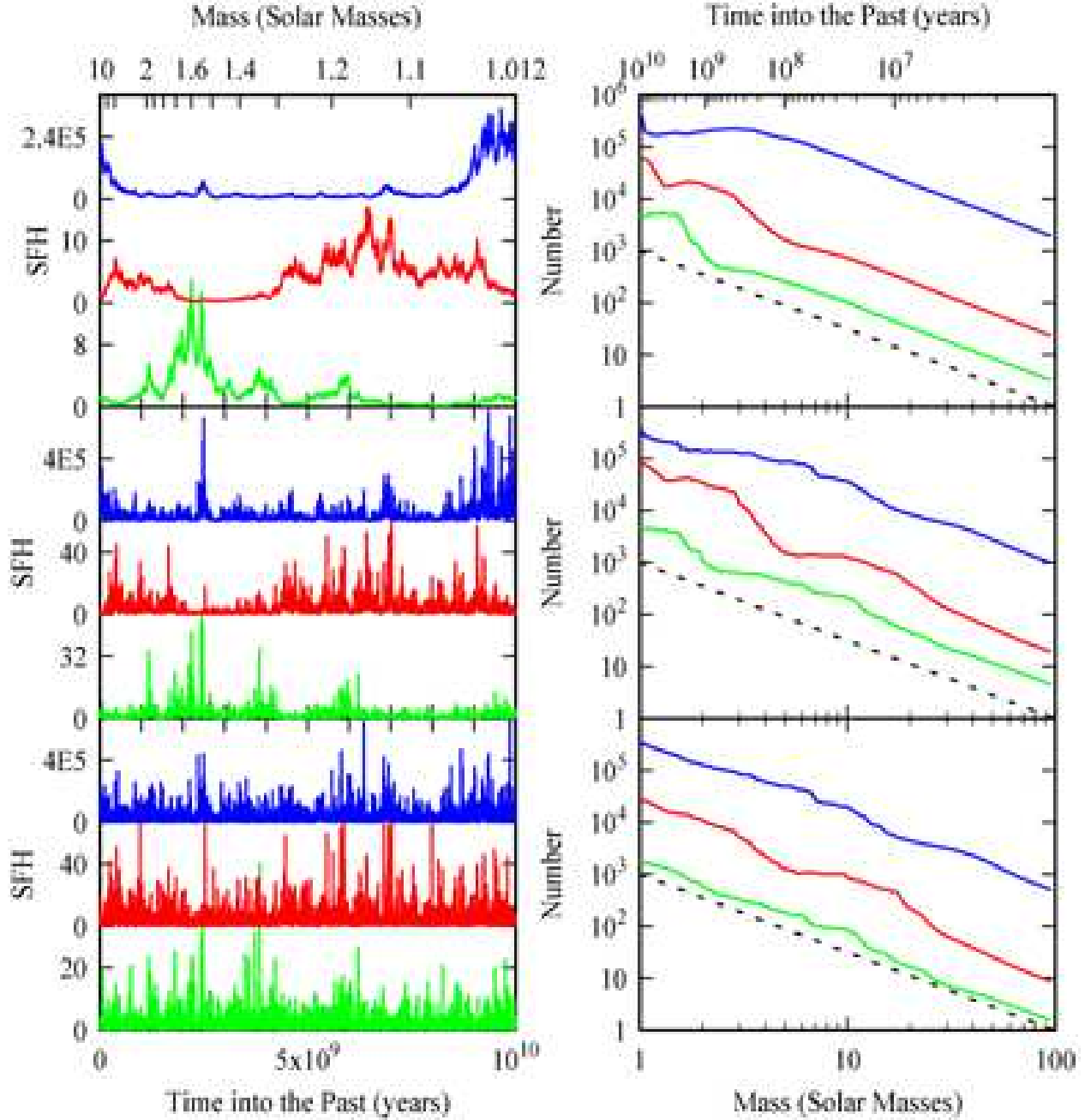


Fig. 2.— Star formation histories (SFH) that have log-normal pdf's and approximate power law power spectra (left) and their associated inferred IMFs (right). Successive plots are shifted upward for clarity. The dotted line on the right has the intrinsic IMF slope of  $\Gamma = -1.5$ . The histories were found by generating noise in Fourier space, multiplying the noise by  $k^{-\beta}$ , taking the inverse Fourier transform, normalizing the resulting Gaussian distribution function of values to an rms dispersion of 1 and an average of 0.1, 1, and 10 (for the lower to upper curves in each panel, respectively), and then exponentiating the result to get a log-normal distribution. Values of  $\beta = 0.25, 0.5$ , and 1 are shown at the bottom, middle and top, corresponding to power spectra of with slopes of  $-0.5, -1$ , and  $-2$ .

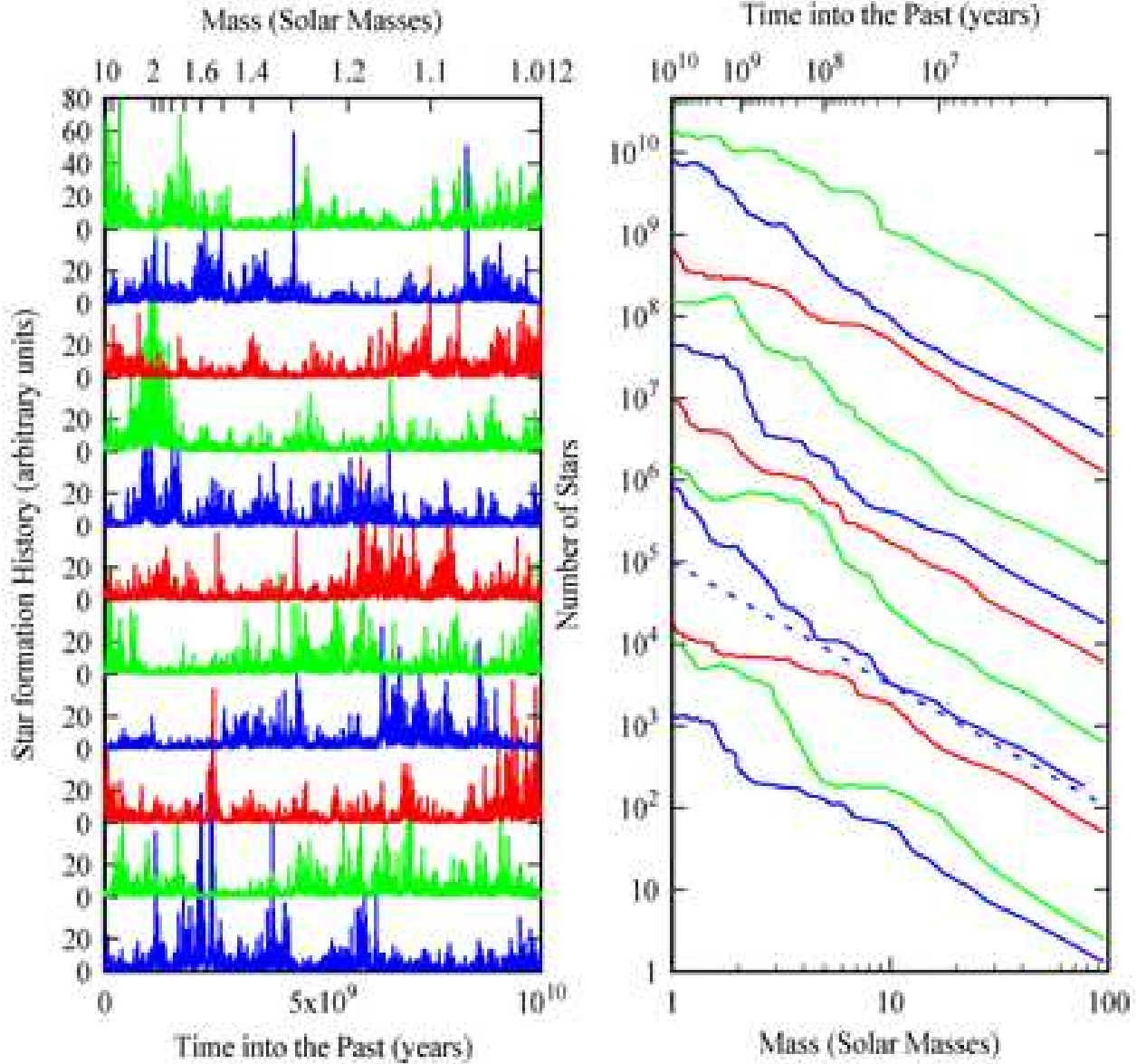


Fig. 3.— Eleven random examples of stochastic star formation histories (SFH) with log-normal pdf's and approximate power law power spectra (left) and their associated inferred IMFs (right). The SFH parameters are the same as in one of the cases in Fig. 2:  $\beta = 0.5$  and an average value before exponentiation equal to 1. Thus, the middle example in the middle panel of Fig. 2 is reproduced here as the second curve up from the bottom in both left and right-hand panels. Successive plots are shifted upward for clarity. The dotted line on the right has the intrinsic IMF slope of  $\Gamma = -1.5$ .

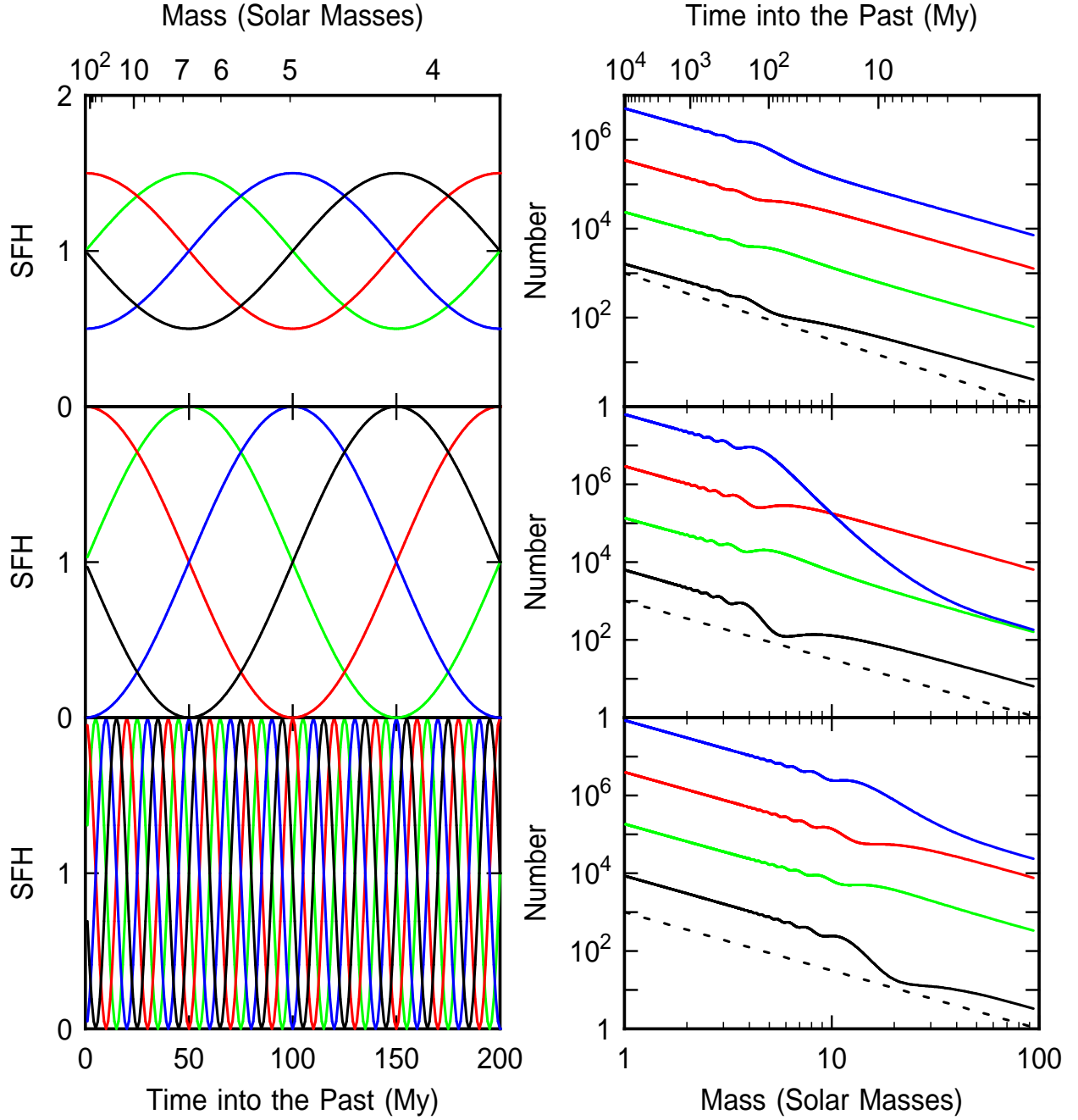


Fig. 4.— Star formation histories that are sine functions with periods of 20 My on the bottom and 200 My in the middle and top panels, along with their inferred IMFs. The minimum values of the SFH are set equal to 0 in the two bottom panels and 0.5 in the top panel. The amplitude of the inferred IMF feature increases with increasing relative amplitude of the SFR variation. The local slope of the IMF depends strongly on the phase of the SFH. The dotted line on the right has the intrinsic IMF slope of  $\Gamma = -1.5$ .

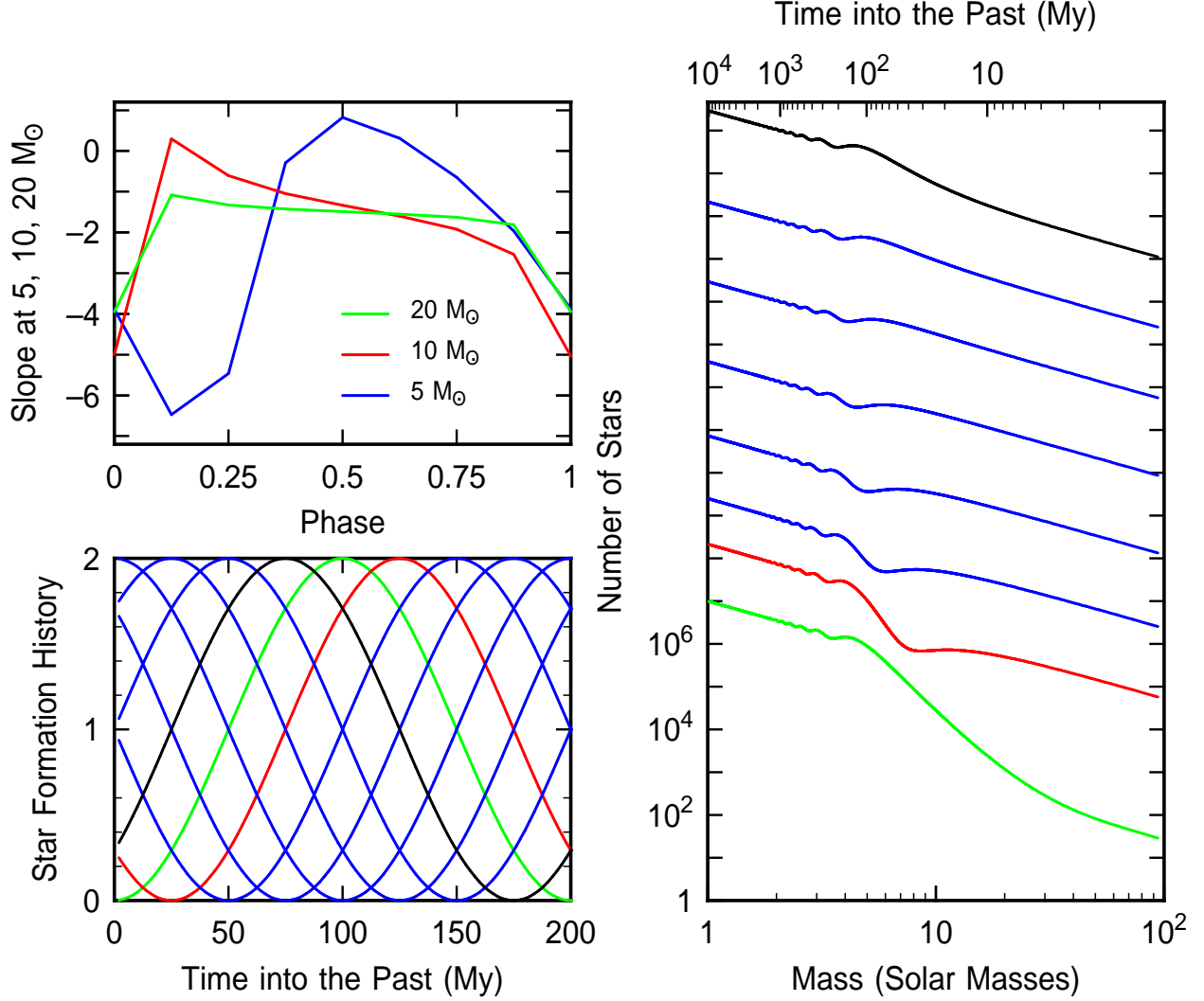


Fig. 5.— Star formation histories are shown in the bottom left panel for eight sine functions with varying phases. The corresponding inferred IMFs are on the right in ascending order (i.e., the SFH that starts at 0 for recent time is shown as the lower IMF). The top left panel shows the inferred IMF slopes  $\Gamma_{infer}$  at three stellar masses, 5  $M_{\odot}$ , 10  $M_{\odot}$ , and 20  $M_{\odot}$ . The slope at each mass is steeper when the SFH has just decreased prior to the time corresponding to the main sequence lifetime at that mass.

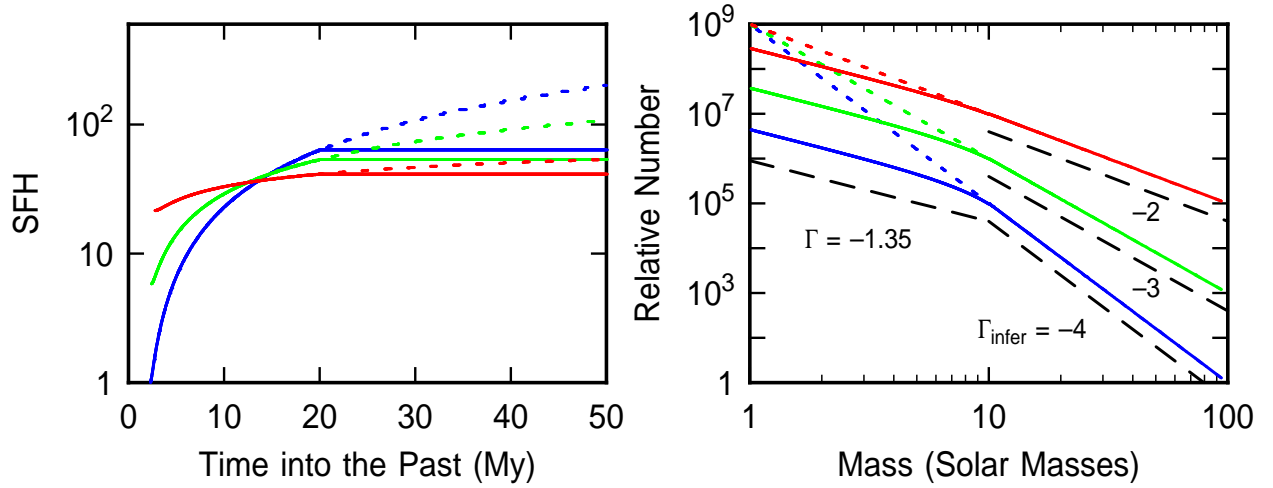


Fig. 6.— Star formation histories (left) that give an inferred IMF with a slope of  $\Gamma_{\text{infer}} = -4$  (blue, with the biggest decline),  $-3$ , and  $-2$  (red, with the smallest decline), as suggested for the field regions of the Large and Small Magellanic clouds. The dashed lines give these slopes down to  $1 M_{\odot}$  and the solid lines give them to  $10 M_{\odot}$ . The resulting IMFs are shown on the right. The intrinsic IMF slope chosen to illustrate these cases is  $\Gamma = -1.35$ .